JVSTA
JOURNAL OF VACUUM SCIENCE AND TECHNOLOGY A

Evolution of sputtered tungsten coatings at high temperature

Veronika Stelmakh, Veronika Rinnerbauer, John D. Joannopoulos, Marin Soljačić, Ivan Celanovic et al.

Citation: J. Vac. Sci. Technol. A **31**, 061505 (2013); doi: 10.1116/1.4817813

View online: http://dx.doi.org/10.1116/1.4817813

View Table of Contents: http://avspublications.org/resource/1/JVTAD6/v31/i6

Published by the AVS: Science & Technology of Materials, Interfaces, and Processing

---

Related Articles

Stability of deflected-beam metal–insulator–metal tunneling cathodes under high acceleration voltage
J. Vac. Sci. Technol. B 31, 042203 (2013)

Simple Si(111) surface preparation by thin wafer cleavage
J. Vac. Sci. Technol. A 31, 023201 (2013)

Novel techniques for modifying microtube surfaces with various periodic structures ranging from nano to microscale
J. Vac. Sci. Technol. B 31, 011806 (2013)

Decomposition and phase transformation in TiCrAlN thin coatings
J. Vac. Sci. Technol. A 30, 061506 (2012)

Surface modification of gold–carbon nanotube nanohybrids under the influence of near-infrared laser exposure
J. Vac. Sci. Technol. B 30, 03D119 (2012)

Additional information on J. Vac. Sci. Technol. A

Journal Homepage: http://avspublications.org/jvsta

Journal Information: http://avspublications.org/jvsta/about/about_the_journal

Top downloads: http://avspublications.org/jvsta/top_20_most_downloaded

Information for Authors: http://avspublications.org/jvsta/authors/information_for_contributors

ADVERTISEMENT

AVS
Advance your technology or engineering career using the **AVS Career Center**, with **hundreds of exciting jobs** listed each month!
http://careers.avs.org

Downloaded 08 Aug 2013 to 18.111.36.116. Redistribution subject to AVS license or copyright; see http://avspublications.org/jvsta/about/rights_and_permissions

Evolution of sputtered tungsten coatings at high temperature

Veronika Stelmakh,[a] Veronika Rinnerbauer, John D. Joannopoulos, Marin Soljačić,
Ivan Celanovic, and Jay J. Senkevich
Institute for Soldier Nanotechnologies, Massachusetts Institute of Technology, Cambridge, Massachusetts 02139

Charles Tucker, Thomas Ives, and Ronney Shrader
Materion Corporation, Buellton, California 93427

(Received 18 April 2013; accepted 25 July 2013; published 8 August 2013)

Sputtered tungsten (W) coatings were investigated as potential high temperature nanophotonic material to replace bulk refractory metal substrates. Of particular interest are materials and coatings for thermophotovoltaic high-temperature energy conversion applications. For such applications, high reflectance of the substrate in the infrared wavelength range is critical in order to reduce losses due to waste heat. Therefore, the reflectance of the sputtered W coatings was characterized and compared at different temperatures. In addition, the microstructural evolution of sputtered W coatings (1 and 5 μm thick) was investigated as a function of anneal temperature from room temperature to 1000 °C. Using *in situ* x-ray diffraction analysis, the microstrain in the two samples was quantified, ranging from 0.33% to 0.18% for the 1 μm sample and 0.26% to 0.20% for the 5 μm sample, decreasing as the temperature increased. The grain growth could not be as clearly quantified due to the dominating presence of microstrain in both samples but was in the order of 20 to 80 nm for the 1 μm sample and 50 to 100 nm for the 5 μm sample, as deposited. Finally, the 5 μm thick layer was found to be rougher than the 1 μm thick layer, with a lower reflectance at all wavelengths. However, after annealing the 5 μm sample at 900 °C for 1 h, its reflectance exceeded that of the 1 μm sample and approached that of bulk W found in literature. Overall, the results of this study suggest that thick coatings are a promising alternative to bulk substrates as a low cost, easily integrated platform for nanostructured devices for high-temperature applications, if the problem of delamination at high temperature can be overcome.
[http://dx.doi.org/10.1116/1.4817813]

I. INTRODUCTION

An on-going interest in solid-state thermal-to-electricity energy conversion concepts, such as thermophotovoltaic (TPV), solar TPV, and solar-thermal energy conversion systems, has led to new investigation and fabrication of refractory metal two-dimensional (2D) photonic crystals (PhCs). These nanostructured surfaces are able to maintain optical and mechanical properties at high temperatures and act as selective emitters to increase the efficiency of the TPV cell. In the emerging field of high-temperature nanophotonics, these metallic 2D PhCs are designed to exhibit precisely tailored optical properties at high temperatures (900 °C and higher) and produce spectrally confined selective emission of light.[1–7] Typically 2D PhCs are fabricated by etching a microscale periodic pattern into a metallic substrate, such as tungsten (W) or tantalum (Ta),[8] which are suitable substrates for PhCs for energy applications due to their high reflectance as well as high melting point and low vapor pressure. Once fabricated, these nanostructured substrates have to be integrated into the TPV system, typically by welding onto the source of heat which can be a microreactor fueled by hydrocarbon combustion[9] or another source of high heat such as radio-isotope fuel cells.[10] The bulk substrate constitutes a high material cost, added thickness resulting in edge parasitic heat loss, with potentially challenging system integration that involves welding or bonding. Additionally, the added weight and thermal expansion coefficient mismatch can be problematic. An integrated PhC thermophotovoltaic system would be advantageous, simplifying the system integration and increasing the fabrication simplicity. Circumventing the problems of bulk W substrates, which are brittle and hard to weld, a W coating could be used as a functional layer on different substrates, selected, and matched to the system's needs, decoupling the requirements of the functional layer and the substrate. Furthermore, such a system would require less material, potentially decreasing the fabrication and postfabrication complexity and integration cost.

In this article, we investigate sputtered refractory metal coatings and their suitability for high-temperature nanostructured devices, thus paving the way toward an integrated combustion,[9,11] radio-isotope,[10] or solar system.[12,13] The key challenges for such coatings are thermomechanical stability regarding delamination, oxide formation, and diffusion at high operating temperatures and achieving long term high-temperature grain stability. In addition, high reflectance is critical for high-temperature nanophotonic devices. In this regime, it is crucial that the substrate has a high reflectance, i.e., low emittance, in the infrared (IR) wavelength range to reduce losses due to waste heat above 2–3 μm.[14] While previous studies of the microstructure, grain growth, resistivity, and stresses in sputtered W films exist,[15,16] they typically do not investigate the optical properties of the films, are limited to relatively low temperatures (20–300 °C), and focus on

---

[a] Electronic mail: stelmakh@mit.edu

thin films (less than 1 μm). The reflectance, grain size, microstrain, and roughness of sputtered coatings of different thicknesses (1 and 5 μm) were quantified in this study and compared as a function of temperature and time from room temperature to 1000 °C. Based on these results, thick coatings are a promising alternative to bulk substrates as a low-cost, easily integrated platform for nanostructured devices for high-temperature applications, if the problem of delamination at high temperature can be overcome.

II. EXPERIMENT

The W coatings studied in this experiment (1 and 5 μm thick) were fabricated via DC magnetron sputtering on silicon (Si) (1 0 0) substrates, using a planetary configuration. Argon (Ar) was used as a sputtering gas at 10 mTorr, with a base pressure of $\sim 8 \times 10^{-7}$ Torr. The chamber contained a heat source that was used to bring the internal chamber and substrates to a temperature of 400 °C. The deposition was carried out at this elevated temperature, which allowed the mobility of the arriving atoms to achieve a dense structured film. Before the deposition, an RF back-sputter was carried out to prepare the substrate for optimal adhesion. The adhesion layer, 100 Å of Titanium (Ti), was deposited at 10 mTorr with no gas modulation. The W deposition was then activated still under elevated temperature (400 °C). During the W metallization, the starting pressure of Ar at 10 mTorr was modulated between 10 and 30 mTorr in increments of 10 min at 10 mTorr and 15 min at 30 mTorr until the desired thickness was achieved. The Ar gas modulation assists in alleviating film stress by obtaining a near neutral stress state of the deposited film. A slight compressive stress to the film is an acceptable condition for adhesion to the substrate.[17,18] The chamber was slowly allowed to cool to ambient temperature before opening.

The prepared samples were imaged by atomic force microscopy (AFM), using the Veeco Nanoscope V Dimension 3100, to characterize the surface and roughness of the samples. A Zeiss scanning electron microscope (SEM) was used to obtain images of the cross-section of the sample and to confirm the film thickness. The reflectance of the W samples was obtained experimentally at room temperature and before and after each annealing run using an automated spectroradiometric measurement system, scanning the wavelength from 1 to 3 μm. The effects of temperature on the samples were studied using two different furnaces. X-ray diffraction (XRD) analysis was performed in the PANalytical X'Pert Pro Multipurpose Diffractometer with an Anton-Paar HTK1200N Furnace *in situ*, in vacuum (50 mTorr), flowing Ar gas (100 mTorr) over a 48 h period while heating at a rate of 5 °C/min to avoid thermal shock. Using this method, the broadening of the W peaks and the microstrain evolution were quantified as a function of temperature, from room temperature to 1000 °C. In order to characterize the optical properties in dependence of each annealing temperature, another set of samples was annealed in a tube furnace in vacuum (10 mTorr base pressure), flowing Ar gas (60 mTorr), at a slow heating and cooling rate of 2 °C/min. The samples were annealed at 500, 700, 800, and 900 °C for 1 h, and reflectance was measured after each annealing run.

III. RESULTS AND DISCUSSION

The coatings were characterized as deposited by AFM and SEM scanning images (Fig. 1). The surface roughness of the two samples was characterized and compared using the AFM. The arithmetic average (R_a) of the roughness was found to be 4.56 and 18.6 nm for a coating thickness of 1 and 5 μm, respectively, with a maximum amplitude range (Z) of 50.7 and 206 nm, respectively. A strong preferential columnar growth was observed in the SEM images of the cross-section of both coatings (Fig. 1), which was observed in literature for W coatings grown under tensile stress.[19]

The optical properties of the coatings as deposited and after annealing at different temperatures were characterized. As mentioned, the reflectance of the substrates, especially in the IR wavelength range is of utmost importance for the intended use as substrates in PhC fabrication and their application in energy conversion. In this application, any emission at long wavelength will lead to additional losses as waste heat. Therefore, the goal is to achieve substrates with high reflectance, i.e., low emittance. The measured spectral reflectance of the unannealed sputtered samples as deposited was not as high as that of bulk W in the IR range and was found to be 0.80 and 0.75 at a wavelength of 2 μm for the 1 and 5 μm sample, respectively, in comparison to 0.9 for bulk W.[20] In order to measure reflectance as a function of annealing temperature, one set of samples was annealed at different temperatures for 1 h each. The 1 μm sample exhibited higher reflectance than the 5 μm sample for all wavelengths before annealing, but its reflectance did not change significantly with annealing up to 700 °C at which point it delaminated. The 5 μm sample annealed at 900 °C, however, showed a significant increase in reflectance, and after a 1 h anneal at 900 °C, the 5 μm sample's reflectance was comparable to the values found in literature for polished flat W (Fig. 2). The increase in reflectance can be attributed to coating densification, decreased porosity of the layer, and grain growth.[21] According to effective medium theory,[22,23] the effective refractive index of a heterogeneous medium depends on the volume fraction of the two constituents and is limited by the Wiener bounds. As the fraction of air respective voids and grain boundaries to metal decreases with annealing in the deposited layers, the effective refractive index increases, leading to higher reflectance. Hence, annealing of the W coatings at temperatures at or above 900 °C is essential in order to obtain the reflectance required for photonic applications at high temperature, for the W sputtering parameters used in this study.

The surface roughness and coating structure of the thicker coating before and after annealing at 900 °C is compared by AFM surface scans and SEM images of the film cross-sections, respectively, in Fig. 3. It was observed that the reflectance of the sample increased after annealing even though the surface roughness also increased from approximately 19 to 35 nm. No visible change in the structure of the

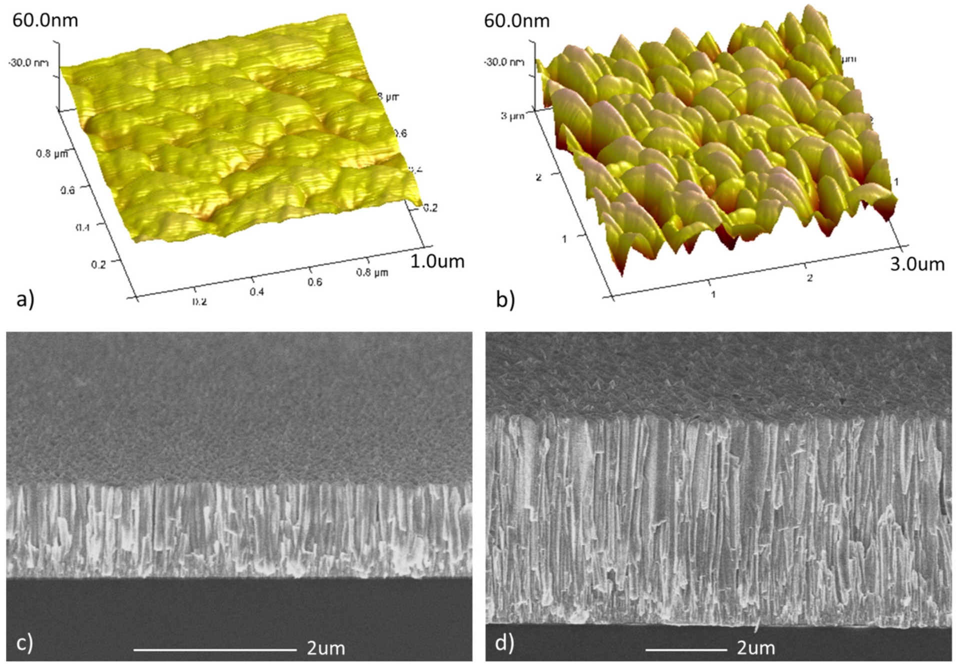

FIG. 1. (Color online) (a) and (c) AFM and SEM imaging, respectively, of the 1 μm W sputtered film. (b) and (d) AFM and SEM imaging, respectively, of the 5 μm W sputtered film, showing increased roughness of the 5 μm thick layer as compared to the 1 μm thick one. Preferential growth is observed in both samples.

W coating and no volume change can be discerned in the cross-section images. The densification of a deposited film during annealing that can be observed in an increase in reflectivity in our study, and more generally in a change of the optical and electrical properties of deposited metal films, does not necessarily lead to a reduction of volume. It is rather a consequence of a reduction of porosity along grain boundaries and a reduction of defect sites that would be reordered at higher temperature and thus release some of the disorder and microstrain accumulated during deposition.[14,21]

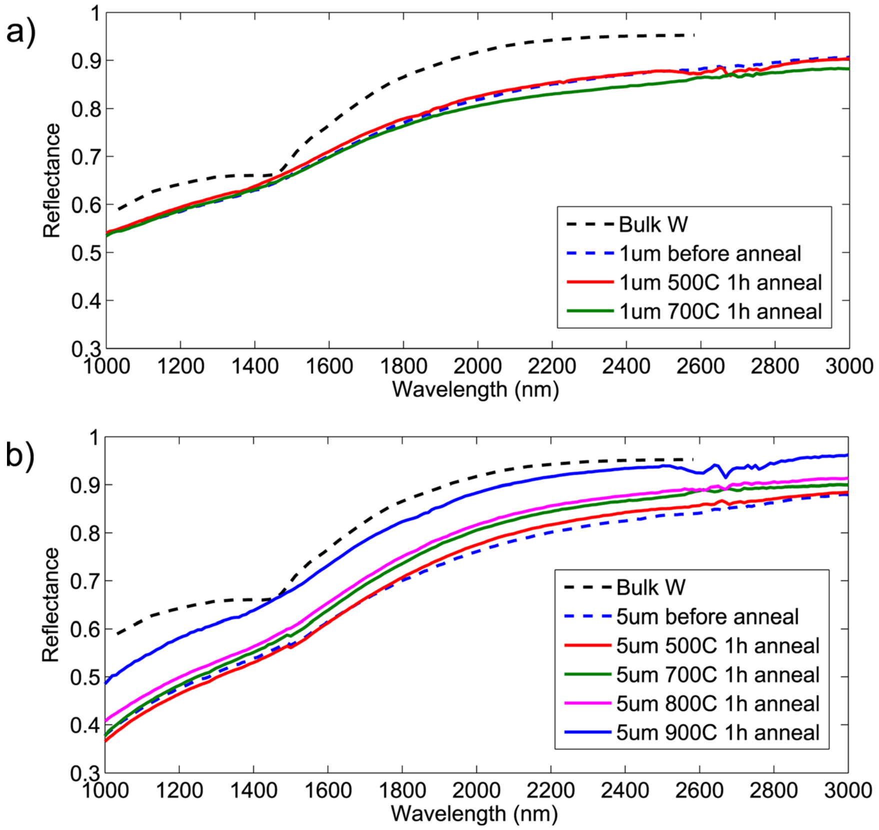

FIG. 2. (Color online) Comparison of reflectance of bulk W (Ref. 20) to the experimentally measured reflectance of (a) the 1 μm sputtered W coating and (b) the 5 μm sputtered W coating before and after the 1 h anneal in a tube furnace at different temperatures at a ramp rate of 2 °C/min.

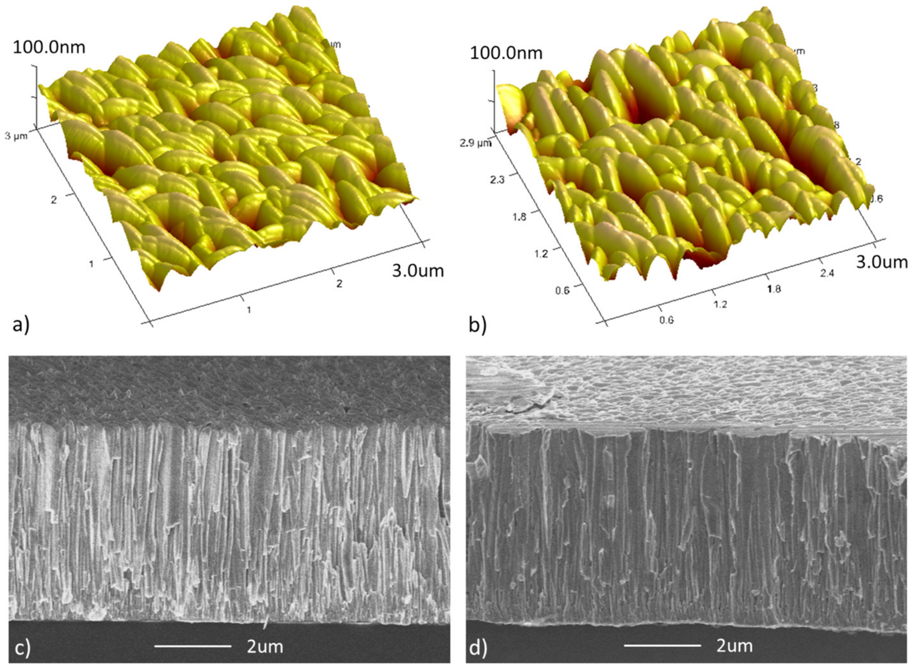

FIG. 3. (Color online) (a) and (c) AFM and SEM imaging, respectively, of the 5 μm W sputtered film before anneal (room temperature). (b) and (d) AFM and SEM imaging, respectively, of the 5 μm W sputtered film after anneal at 900 °C for 1 h. No noticeable difference in thickness was observed after anneal despite an increase in roughness.

The approximate crystallite size and microstrain (nonuniform lattice strain) of the samples was determined by evaluating the broadening of the diffraction peaks in the XRD pattern. Generally, in a powder sample, a large number of diffraction peaks is obtained. In the case of our coatings, only two W peaks were observed: the (1 1 0) peak and the (2 2 0) peak, as shown in Fig. 4, which is attributed to the highly textured nature of the sputtered samples due to a strong preferential growth. The microstrain in the samples was quantified using the Williamson-Hall plot.[24] Since the broadening of the peaks was dominated by microstrain, the crystallite size was not easily resolved. It was found to be between 50 and 100 nm for the 5 μm sample and 20 and 80 nm for the 1 μm sample at room temperature, before anneal. The lack of precision was due to the presence of only one first-order peak resulting in microstrain dominance. A crystallite size of 10–50 nm range has previously been observed in W sputtered thin-films deposited at room temperatures[15] which is in the same range as our findings.

Our thick W coatings were sputtered by stress balancing them by modulating an Ar gas pressure between 10 and 30 mTorr. Quite possibly the 10 mTorr layer and the 30 mTorr layer have different grain structure and physical density; however, each layer was not independently investigated. Instead, the composite coating was characterized. It is essential to balance the stress in such thick coatings in order to avoid delamination. The influence of the deposition conditions on the

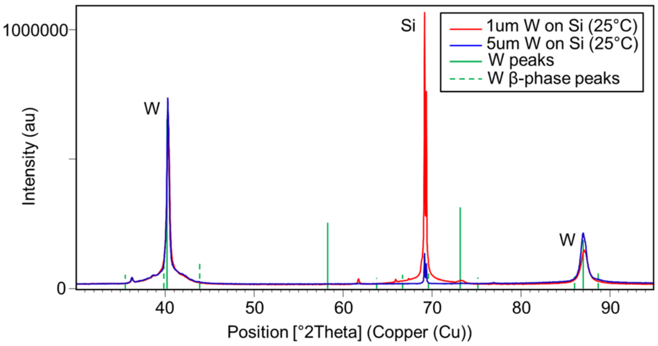

FIG. 4. (Color online) XRD data collected using a diffracted beam monochromator. The 1 and 5 μm W films deposited on a Si (1 0 0) substrate are compared at 25 °C. The predominant peak of the Si occurring at 69.3° corresponds to the (1 0 0) peak. The predominant peak of the W occurring at 40.2° corresponds to the (1 1 0) peak, and the other significant W peak occurring at 86.9° corresponds to the higher order peak (2 2 0). The presence of only one first order peak indicates the highly textured nature of the W sample. The small peak at 36.2° 2θ can be readily identified as copper K-β peak due to the XRD source, not the W coating. No W β-phase peaks are present.

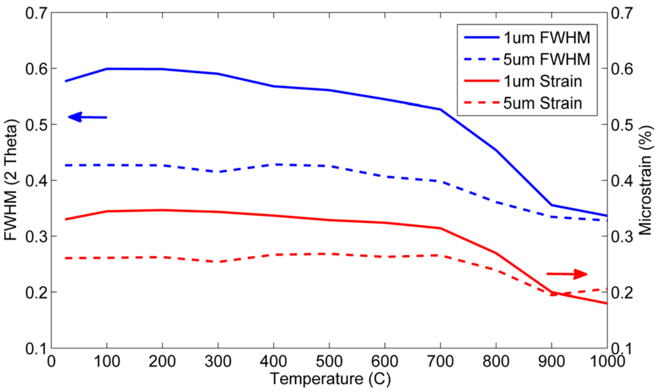

FIG. 5. (Color online) Left axis: FWHM of the 1 and 5 μm W sample as a function of temperature. Right axis: microstrain of the 1 and 5 μm W sample as a function of temperature. While the exact crystallite size could not be determined, the crystallite size of the 5 μm sample was clearly larger resulting in a smaller FWHM of the diffraction peak.

properties of DC magnetron sputtered thin W films is well studied.[19] Depending on Ar gas pressure, substrate material, substrate temperature, and deposition duration, there is a different relative amount of beta- and alpha-W phase deposit. According to literature,[25–27] the beta phase is metastable and transforms into alpha phase. It is a thermally driven process but the transformation takes place even at room temperature. For thicker films (>50 nm), even deposited at room temperature, no beta phase is found.[25,26] This is confirmed in Fig. 4 as no W beta phase peaks were found in the XRD analysis of the thick W coatings.

In order to quantify the evolution of the microstrain as a function of temperature, an *in situ* XRD analysis was performed on the 1 and 5 μm samples over a 48 h period from 25 to 1000 °C in 100 °C increments. For each temperature, the diffraction peak width at full width half-maximum (FWHM) and microstrain were quantified (Fig. 5). A clear inflection point was seen around 700 °C for both the 1 and 5 μm samples. Assuming that the majority of the peak broadening was due to microstrain, as in the room temperature measurements, the results indicated that the microstructure was unambiguously changing. The microstrain was quantified, ranging from 0.33% to 0.18% for the 1 μm sample and 0.26% to 0.20% for the 5 μm sample, decreasing as the temperature increased. This observation is reasonable since at higher temperatures, molecular mobility increases and thus lattice strain is relieved. It was observed that the 5 μm sample had less microstrain than the 1 μm sample at all temperatures.

The tensile stress in the films is attributed to the coefficients of thermal expansion (CTE) mismatch of substrate and film and the elevated substrate temperature during deposition. The films were deposited at an elevated temperature of 400 °C and the deposition parameters were chosen such that the films were mostly balanced at the deposition temperature. As the substrates cool down after deposition, however, the smaller CTE of the substrate leads to an increasingly tensile stress in the coatings. Therefore, as the samples are annealed, the tensile stress is released again, which can be seen in the reduction of the tensile microstrain with increasing temperature.

Despite the decrease in microstrain (i.e., decrease in the number of dislocations and defects in the film) with increasing temperature, delamination occurred between 700 and 800 °C for the 1 μm sample and between 900 and 1000 °C for the 5 μm sample after annealing in the tube furnace. The delamination can be attributed to the mismatch in CTE of Si and W. The linear CTE of Si is about 2.6×10^{-6}/°C, while the CTE of W is about 4.6×10^{-6}/°C.[28] Differences in the CTE values of adjacent materials during heating and cooling will induce tensile stress in W, leading to cracks in W, since it is a brittle material and cannot withstand tensile stresses. In the case of a brittle material like W, the CTEs should be matched within about 0.2×10^{-6}/°C and a mismatch of 0.5 to 1.0×10^{-6}/°C is considered the upper limit.[29,30] In addition, the CTE of Ti is about twice as high as that of W and could therefore play an additional role in the delamination. However, since the 100 Å layer of Ti used as an adhesion layer represents only 1% of the total thickness of the 1 μm film and only 0.2% of the thickness of the 5 μm film, the thermal mismatch of the CTE of Ti was considered to be a minor effect in the annealing behavior. While the 5 μm sample did not delaminate when annealed at 900 °C, it did begin to show signs of microscopic cracking.

IV. CONCLUSION

In thermophotovoltaic applications, bulk W substrate PhCs are brittle and hard to weld. An integrated PhC thermophotovoltaic system would require less material, potentially decreasing the fabrication and postfabrication complexity and integration cost. Using a W coating as a functional layer on different substrates, selected and matched to the system's needs, would decouple the requirements of the functional layer and the substrate.

The properties of W coatings, in particular the optical properties, microstrain and surface roughness, and their evolution at high temperatures, were studied as a potential fabrication route for high-temperature nanostructured surfaces. The 5 μm thick layer was found to be rougher than the 1 μm thick layer which resulted in a lower reflectance at room temperature at all wavelengths. However, after annealing the 5 μm sample at 900 °C for 1 h, its reflectance exceeded that of the 1 μm sample and came very close to that of bulk W found in literature. An XRD analysis was conducted to understand the effect of temperature on the crystallite size and microstrain of the 1 μm and 5 μm samples. The grain growth could not be definitively quantified due to the dominating presence of microstrain in both samples but was in the order of 20 to 80 nm for the 1 μm sample, and 50 to 100 nm for the 5 μm sample, as deposited, and increased with temperature. Microstrain was quantified, ranging from 0.33% to 0.18% for the 1 μm sample and 0.26% to 0.20% for the 5 μm sample, decreasing as the annealing temperature increased especially for temperatures greater than 700 °C. It was observed that the 5 μm sample had less strain and larger crystallite size than the 1 μm sample at all temperatures.

The delamination of the W at high annealing temperature was attributed to the mismatch in CTE of Si and W and will be further studied using different substrates. In addition, different sputtering processes, resulting in denser sputtered coatings potentially leading to higher reflectance, are currently being investigated. Tantalum, a less brittle and more compliant material, that would have similar optical properties to W, will also be studied in the future as an approach to sputtered high-temperature high-reflectance coatings for 2D photonic crystals.

Overall, the results of this study suggest that sputtered W layers are a promising approach to a high-temperature, high reflectance coating for a PhC substrate, if the challenge of delamination at high temperatures can be overcome.

ACKNOWLEDGMENTS

XRD analysis was performed at the MIT Center for Materials Science and Engineering XRD SEF. The authors thank Scott Speakman for his help with XRD analysis and insightful conversations. This work was partially supported by the Army Research Office through the Institute for Soldier Nanotechnologies under Contract Nos. DAAD-19-02-D0002 and W911NF-07-D000. M.S. was partially supported by the MIT S3TEC Energy Research Frontier Center of the Department of Energy under Grant No. DE-SC0001299. V.R. was funded by the Austrian Science Fund (FWF): J3161-N20.

[1] V. Rinnerbauer, S. Ndao, Y. X. Yeng, W. R. Chan, J. J. Senkevich, J. D. Joannopoulos, M. Soljačić, and I. Celanovic, Energy Environ. Sci. **5**, 8815 (2012).

[2] Y. X. Yeng, M. Ghebrebrhan, P. Bermel, W. R. Chan, J. D. Joannopoulos, M. Soljačić, and I. Celanovic, Proc. Natl. Acad. Sci. U.S.A. **109**, 2280 (2012).

[3] M. Araghchini, Y. X. Yeng, N. Jovanovic, P. Bermel, L. A. Kolodziejski, M. Soljacic, I. Celanovic, and J. D. Joannopoulos, J. Vac. Sci. Technol. B **29**, 061402 (2011).

[4] E. Rephaeli and S. Fan, Appl. Phys. Lett. **92**, 211107 (2008).

[5] I. Celanovic, N. Jovanovic, and J. Kassakian, Appl. Phys. Lett. **92**, 193101 (2008).

[6] H. Sai and H. Yugami, Appl. Phys. Lett. **85**, 3399 (2004).

[7] A. Heinzel, V. Boerner, A. Gombert, B. Blsi, V. Wittwer, and J. Luther, J. Mod. Opt. **47**, 2399 (2000).

[8] V. Rinnerbauer, S. Ndao, Y. Xiang Yeng, J. J. Senkevich, K. F. Jensen, J. D. Joannopoulos, M. Soljačić, I. Celanovic, and R. D. Geil, J. Vac. Sci. Technol. B **31**, 011802 (2013).

[9] W. R. Chan, P. Bermel, R. C. N. Pilawa-Podgurski, C. H. Marton, K. F. Jensen, J. J. Senkevich, J. D. Joannopoulos, M. Soljačić, and I. Celanovic, Proc. Natl. Acad. Sci. U.S.A. **110**, 5309 (2013).

[10] C. J. Crowley, N. A. Elkouh, S. Murray, and D. L. Chubb, AIP Conf. Proc. **746**, 601 (2005).

[11] M. Zenker, A. Heinzel, G. Stollwerck, J. Ferber, and J. Luther, IEEE Trans. Electron Devices **48**, 367 (2001).

[12] N. P. Sergeant, M. Agrawal, and P. Peumans, Opt. Express **18**, 5525 (2010).

[13] A. S. Vlasov, V. P. Khvostikov, O. A. Khvostikova, P. Y. Gazaryan, S. V. Sorokina, and V. M. Andreev, AIP Conf. Proc. **890**, 327 (2007).

[14] V. Rinnerbauer, J. J. Senkevich, J. D. Joannopoulos, M. Soljačić, I. Celanovic, R. R. Harl, and B. R. Rogers, J. Vac. Sci. Technol. A **31**, 011501 (2013).

[15] P. Petroff, T. T. Sheng, A. K. Sinha, G. A. Rozgonyi, and F. B. Alexander, J. Appl. Phys. **44**, 2545 (1973).

[16] A. M. Haghiri-Gosnet, F. R. Ladan, C. Mayeux, H. Launois, and M. C. Joncour, J. Vac. Sci. Technol. A **7**, 2663 (1989).

[17] T. Karabacak, C. R. Picu, J. J. Senkevich, G.-C. Wang, and T.-M. Lu, J. Appl. Phys. **96**, 5740 (2004).

[18] T. Karabacak, J. J. Senkevich, G.-C. Wang, and T.-M. Lu, J. Vac. Sci. Technol. A **23**, 986 (2005).

[19] Y. G. Shen, Y. W. Mai, Q. C. Zhang, D. R. McKenzie, W. D. McFall, and W. E. McBride, J. Appl. Phys. **87**, 177 (2000).

[20] E. Palik, *Handbook of Optical Constants of Solids Five-Volume Set* (Academic, San Diego, CA, 1998).

[21] A. W. Sood, D. J. Poxson, F. W. Mont, S. Chhajed, J. Cho, E. F. Schubert, R. E. Welser, N. K. Dhar, and A. K. Sood, J. Nanosci. Nanotechnol. **12**, 3950 (2012).

[22] D. E. Aspnes, Am. J. Phys. **50**, 704 (1982).

[23] O. Wiener, Abh. Math.-Phys. Kl. Saechs. Akad. Wiss. **32**, 509 (1912).

[24] H. Klug and L. Alexander, *X-Ray Diffraction Procedures for Polycrystalline and Amorphous Materials* (John Wiley & Sons, Hoboken, 1974).

[25] I. C. Noyan, T. M. Shaw, and C. C. Goldsmith, J. Appl. Phys. **82**, 4300 (1997).

[26] S. M. Rossnagel, I. C. Noyan, and J. C. Cabral, J. Vac. Sci. Technol. B **20**, 2047 (2002).

[27] I. Djerdj, A. M. Tonejc, A. Tonejc, and N. Radic, *22nd European Crystallographic Meeting ECM22* (Budapest, 2004), Acta Cryst. **A60**, s44 (2004).

[28] J. Groza and J. Shackelford, *Materials Processing Handbook* (CRC, Boca Raton, 2007).

[29] R. G. Frieser, Electrocomponent Sci. Technol. **2**, 163 (1975).

[30] J. Partridge, *Glass-to-Metal Seals, Monographs on Glass Technology* (Society of Glass Technology, Sheffield, 1949).